Pulse-height defect in single-crystal CVD diamond detectors

O. Beliuskina, A.O. Strekalovsky, A.A. Aleksandrov, I.A. Aleksandrova, H.M. Devaraja, C. Heinz, S. Heinz, S. Hofmann, S. Ilich, N. Imai, et al.

Pulse-height defect in single-crystal CVD diamond detectors

O. Beliuskina[1], A.O. Strekalovsky[2], A.A. Aleksandrov[2], I.A. Aleksandrova[2], H.M. Devaraja[3], C. Heinz[4], S. Heinz[4,5], S. Hofmann[5], S. Ilich[2], N. Imai[1], D.V. Kamanin[2], M. Kis[5], G.N. Knyazheva[2], C. Kozhuharov[5], E.A. Kuznetsova[2], J. Maurer[5], G.V. Mishinsky[2], M. Pomorski[6], Yu.V. Pyatkov[2], O.V. Strekalovsky[2], M. Träger[5], V.E. Zhuchko[2]

1 Center for Nuclear Study, The University of Tokyo, Hirosawa 2-1, Wako, Saitama 351-0198, Japan, e-mail: o.beliuskina@cns.s.u-tokyo.ac.jp
2 Flerov Laboratory of Nuclear Reactions, JINR, Dubna, Moscow Region, Russia
3 Manipal Centre for Natural Sciences, Manipal University, Manipal 576014, Karnataka, India
4 Justus-Liebig-Universität Gießen, II. Physikalisches Institut, Heinrich-Buff-Ring 16, 35392 Gießen, Germany
5 GSI Helmholtzzentrum für Schwerionenforschung, 64291 Darmstadt, Germany
6 CEA, LIST, Diamond Sensor Laboratory, CEA/Saclay, 91191 Gif-sur-Yvette, France

Abstract

The pulse-height *versus* deposited energy response of a single-crystal chemical vapor deposition (scCVD) diamond detector was measured for ions of Ti, Cu, Nb, Ag, Xe, Au, and of fission fragments of ^{252}Cf at different energies. For the fission fragments, data were also measured at different electric field strengths of the detector. Heavy ions have a significant pulse-height defect in CVD diamond material, which increases with increasing energy of the ions. It also depends on the electrical field strength applied at the detector. The measured pulse-height defects were explained in the framework of recombination models. Calibration methods known from silicon detectors were modified and applied. A comparison with data for the pulse-height defect in silicon detectors was performed.

1 Introduction

The response of semiconductor detectors to the energy lost by swift heavy ions is complicated due to the fact that the kinetic energy of the ion is not completely converted into an electric signal. The emerging pulse-height defect (PHD) depends on the energy, mass, and charge of the ion and also from the detector properties. The PHD is defined as the energy difference ΔE between the kinetic energy E_k of an ion incident on the surface of a detector and the apparent energy E_{DD} derived from the measured electric signal:

$$\Delta E = E_k - E_{DD} \quad (1)$$

The PHD is almost negligible for protons or α particles for energies beyond several MeV.

Most detailed studies of PHD were performed for Si detectors [1–6]. Another promising detector material is he chemical vapor deposition diamond (CVD) [7,8]. The CVD material is grown in a chemical vapor deposition process. Details of the manufacturing process are given in [9]. It appears that this material extends the possible applications for heavily-ionizing particles compared to Si. Table 1 lists the relevant material parameters and compares them with those for silicon.

Physical properties at 300K	Diamond	Silicon
Atomic charge	6	14
Density / (g cm^{-3})	3.5	2.33

Lattice constant / Å	3.57	5.43
Band gap / eV	5.45	1.12
Intrinsic carrier density / cm^3	$< 10^3$	1.5×10^{10}
Energy to create e-h pair / eV	13	3.6
Thermal conductivity / (W cm^{-1} K^{-1})	20	1.27
Thermal expansion coefficient / K	0.8×10^{-6}	2.6×10^{-6}
Resistivity / (Ωcm)	$>10^{11}$	2.3×10^5
Breakdown field / (V/cm)	10^7	3×10^5
Electron mobility / (cm^2/Vs)	2200	1500
Hole mobility / (cm^2/Vs)	1600	600
Saturation velocity / (km/s)	220	82
Dielectric constant	5.7	11.9

Table 1. Basic properties of intrinsic diamond and silicon.

Some characteristics of scCVD diamond detectors, in the following abbreviated as DD, are superior to the properties of Si detectors. *E.g.*, they reveal fast timing behavior and large radiation hardness while the energy resolution of $\sim 0.3\%$ for 5 MeV α particles is comparable to that of Si detectors [7,10,11]. In addition, the charge collection for fully-ionized relativistic heavy ions was found to be close to 100% [12].

The use of DDs as detectors for low-energetic heavy ions is still at its beginning. There are only few publications about PHD in DD [13–15]. Sato *et al.* [13,14] have studied the pulse-height reduction effect for low-energy heavy ions Cu, Au, Si, and C at 3 MeV. The PHD was found to be significantly larger compared to Si detectors. *E.g.*, in their measurements the output pulse height of Si surface barrier detectors for Au ions is approximately half of that of α particles at the energy of ~ 7 MeV and even smaller was the output pulse height of DD for Au where only one tenth of that of protons was measured at incident energies of 3 MeV. Due to the measurements at different energies, the results cannot be compared directly. The use of DD as fission fragment detectors was studied in [15]. The authors concluded that all their DDs show inadequate energy resolution and suffer from an extensive PHD. The detected pulse height never exceeded about 30% of what they expected from a simulation of the stopping of fission fragments in DD.

Applications like ΔE-E-ToF telescopes might be a conceivable option as detection system for heavy lowenergetic reaction products if the usually used Si detectors or ionization chambers are replaced by diamonds [16]. ΔE-E-ToF telescopes are widely used in heavy ion reaction studies to determine the mass and proton number, A and Z, of the reaction products. In collisions near the Coulomb barrier, they are frequently applied to study the A and Z distributions of reaction products from deep inelastic transfer, quasi-fission and fusion-fission reactions in very heavy systems up to $^{238}U + ^{238}U$ [17]. The fast timing properties of diamond detectors would allow the use of diamonds in a telescope simultaneously for energy and ToF measurement. The conventional MCP detectors for ToF determination could be replaced. Further, the large radiation hardness of diamond detectors would allow to position the telescope arms at small forward angles. Detector arms using Si detectors usually have to be installed at angles larger than 20 degrees to prevent damage of the detectors at high rates of elastically scattered ions.

However, the critical point in applications of DDs in low-energy heavy ion physics is the PHD. *E.g.*, it determines the mass resolution which can be obtained for the reaction products if they are identified via ToF-E measurements [18,19]. Typically, the mass resolution is not

better than 3 atomic mass units. Disadvantageous is also the small size of DDs. A maximum size of 4.5 × 4.5 mm^2 can be manufactured for a single crystal at a thickness of 500 μm. Only a few companies succeeded to produce crystals for energy measurements.

The objective of our work is to investigate PHD in DD as a function of beam energy and ion type and to obtain a reliable and convenient practical guide for the determination of energy calibration parameters for diamond detectors, which depend on A and Z of the stopped ions. Only with the knowledge of the response of the detector to various ions and energies, unknown ions can be identified in an experiment. The calibration procedures are performed within the framework of methods developed for Si detectors [1–6]. The investigations were performed at ion energies in the range (20–90) MeV. The energies of heavy reaction products emerging from nuclear collisions at the Coulomb barrier are typically located in this energy range.

2 Experimental setup

The experiment was carried out at the IC-100 cyclotron at the Flerov Laboratory of Nuclear Reactions (FLNR) of the Joint Institute for Nuclear Research (JINR) in Dubna, Russia. The ions to be studied were produced in elastic collisions of a ^{132}Xe beam with the selected target material. The ^{132}Xe beam had an average intensity of $\sim 10^{12}$ particles/s. The incident ion energy was about 130 MeV. Targets of natural Ti, Cu, Nb, Ag, and Au with thicknesses of $\sim$ 1.5 μm were irradiated. In the case of the isotopically mixed targets Ti, Cu, and Ag, mass numbers 48.3, 64.4, and 108.0, respectively, were used in the data analysis. These masses were determined as weighted mean values of the masses of the naturally abundant isotopes.

Elastically scattered target and projectile ions were measured with a DD manufactured at the GSI detector laboratory. A CVD diamond single crystal was produced by the company Element Six [20]. The detector diameter was 2.7 mm with a thickness of 100 μm. Thin layers of aluminium with thicknesses of 100 nm are evaporated on both sides acting as Schottky electrodes for applying the electric voltage. A sketch of the experimental setup is presented in fig. 1. The diamond detector was installed at an angle of 30° relative to the beam direction at a distance of 711 mm from the target. The detector covered a solid angle of 1.13×10^{-5} sr.

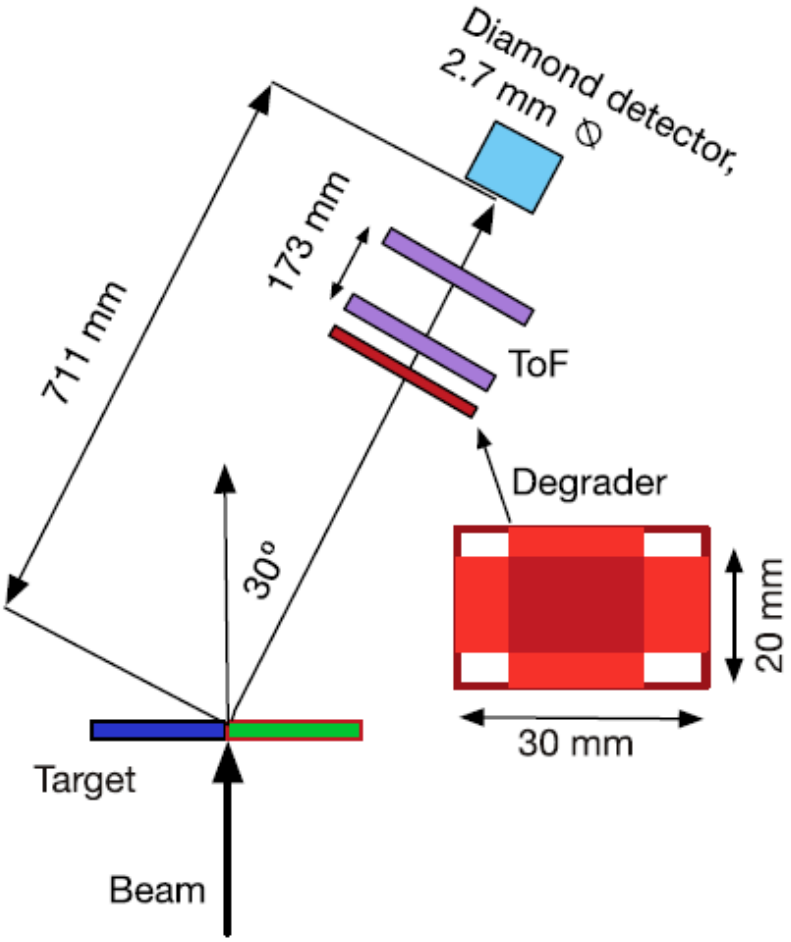

Fig. 1. Sketch of the experimental setup. For details see text

In front of the DD, two secondary electron ToF detectors were installed to determine the kinetic energy of the scattered ions. The detectors consisted of a polycarbonate foil (Lexan-Macrofol) of 30 μg/cm^2 thickness covered downstream with 40 μg/cm^2 gold. The foil was mounted on a frame with a 20 mm × 30 mm square opening. An electrostatic mirror (grid) deflected the electrons emitted in beam direction onto a stack of two micro-channel plates (MCP) in series. Each MCP had a diameter of 32 mm and a thickness of 0.3 mm. The distance between the ToF detectors was 173 mm and that of the second ToF detector and the DD was 40 mm. The ToF measurement was calibrated with α particles from a ^{226}Ra source.

Because of the limited beam time, we irradiated two target materials simultaneously. For this purpose, the target frame of 20 mm × 30 mm was divided into two equal parts of 20 mm × 15 mm. The targets of Ti and Cu and that of Nb and Ag, respectively, were irradiated simultaneously and, eventually, a single Au target was used.

A degrader was installed in front of the first ToF detector at a distance of about 10 mm. Size and arrangement of the degrader foils are shown in fig. 1. Two crossed Ti strips with thicknesses of 1 μm were mounted, which allowed to measure simultaneously three different energies, the undegraded ions when they passed through the holes in the degrader and two degraded ones when the ions passed the areas covered with the Ti foils of 1 and 2 μm thickness. The energy of the undegraded target ions is given by the energy after elastic scattering in collisions with the Xe beam into the angle of 30°. The reason for a low count rate at the highest energy is that the total blank area is smaller than those of 1 and 2 μm degrader

foils. In the case of irradiations of the combined Nb and Ag targets, the irradiation time was too short so that the number of counts was insufficient for determining the peak at the highest energy.

For the errors of measured values of kinetic and deposited energies the standard deviations $\pm\sigma$ were used. The PHD errors were determined as square root of the sum of the quadratic errors of the kinetic energy E_k and apparent energy E_{DD}. The main part of the energy uncertainty is due to the energy distribution of the ions in the finite target thickness. The ToF-distance uncertainty equals to ±1 mm which corresponds to ±1 %. The energy resolution of the diamond detector including the contribution from the readout electronics was around 2% for alphas of ^{226}Ra and considered as the same value for heavy ions. The kinetic energy error resulting from the use of the weighted mean mass number instead of the actual values is small. The solid angle covered by the diamond detector is small therefore the angle straggling and re-scattering on the degrader are negligible. The scattering angle in the ToF foil is about 5.4°. Concerning the determination of the energy, this effect is irrelevant because the energy is measured between the two foils of the ToF detectors.

The energy calibration was performed with α particles from a ^{226}Ra source which has energies of 4.772, 5.490, 6.002, and 7.682 MeV. The calibration of the electronics up to the highest energy of 90 MeV was performed with a precision pulser. Assuming no PHD for α particles, this calibration method for the signals of heavy ions stopped in DD is a direct measurement of the energy of the ions converted into an electric signal. The difference to the also measured kinetic energy by the ToF detectors results in the PHD.

The PHD *versus* kinetic energy was measured for Ti, Cu, Nb, Ag, Xe, and Au ions in the energy range from 20 to 90 MeV at a constant electric field of 2V/μm, which is typical for scCVD diamond detectors. For fission fragments of a ^{252}Cf source, the PHD was also investigated at different field settings. Values in the range (0.7–2.5) V/μm were used. For all measurements of the fission fragments, the ^{252}Cf source was placed directly in front of the DD at a distance of 27 mm.

3 Experimental results

An example for the measured data from the irradiation of the combined Ti and Cu target with ^{132}Xe ions at the electric field of 2 V/μm is shown in fig. 2. The data were taken during a measuring time of 1 hour. The two-dimensional scatter plot shows the deposited energy of the ions measured with DD *versus* their kinetic energy measured with the ToF detector.

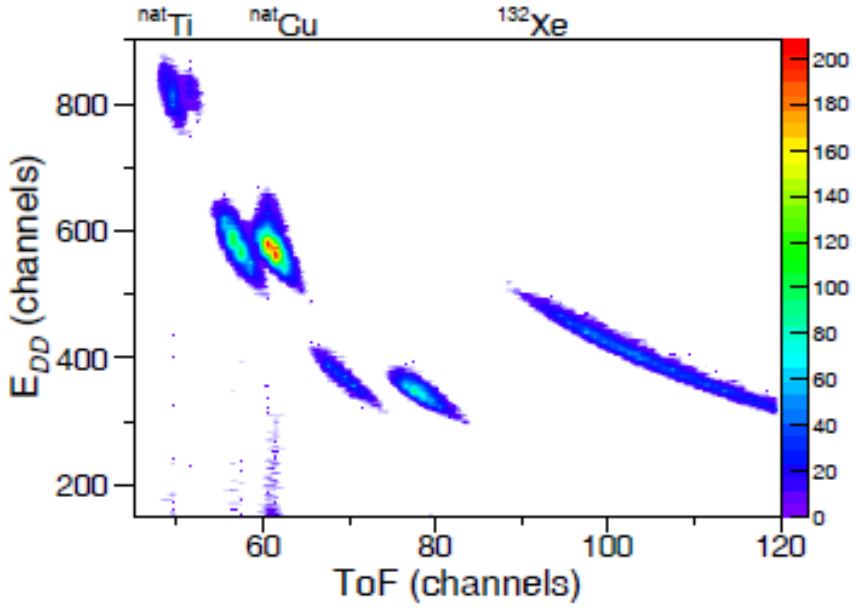

Fig. 2. Two-dimensional spectrum of energies E_{DD} derived from the diamond detector *versus* ToF for ^{nat}Ti, ^{nat}Cu, and ^{132}Xe measured at an applied electric field strength of 2 V/μm. The three clusters of points for ^{nat}Ti and ^{nat}Cu are, from top to bottom, due to the ions passing through the holes, the 1 μm and 2 μm thick Ti foils, respectively, of the degrader mounted in front of the ToF detectors.

The two branches in the left each consisting of three energy peaks are due to Ti (most left) and Cu ions. The third branch in the right is due to scattered ^{132}Xe ions. The projections of the data points of the Ti branch on the ToF axis and the axis of the energy measured with DD are shown in fig. 3. The different height of the peaks is due to the different sizes of the areas of the degrader and the different scattering conditions as explained before.

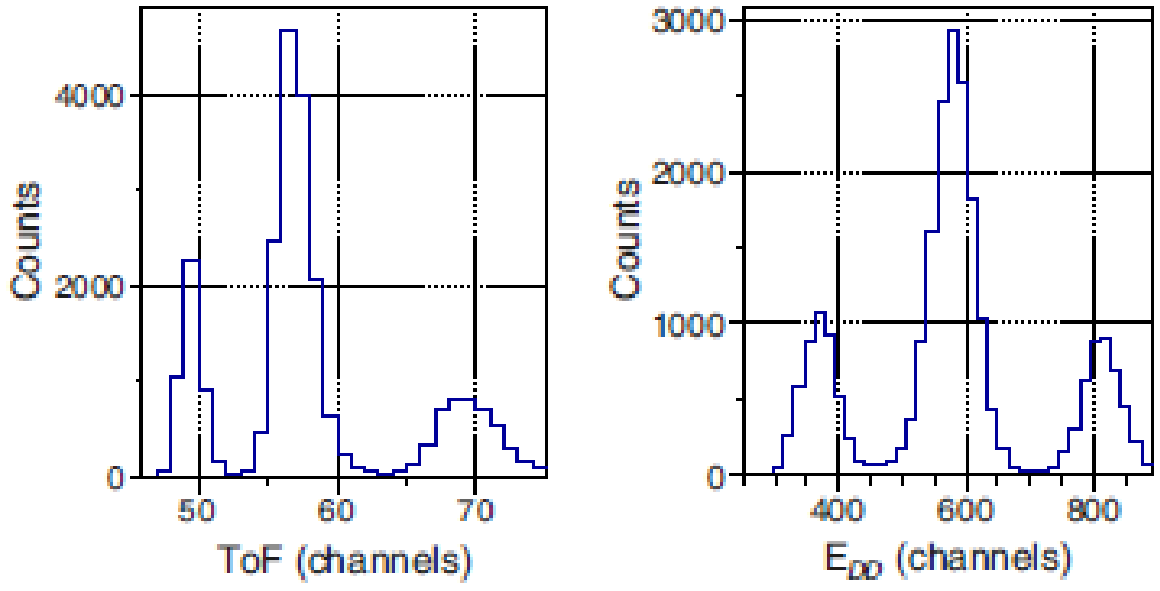

Fig. 3. Energy spectra of Ti ions. The left panel shows the time-of-flight spectrum, and the right panel shows the energy E_{DD} measured by the diamond detector.

Ion	Z	A	E_k	E_{DD}	ΔE	ΔE_w	ΔE_n	ΔE_r
Ti	22	48.3	60.3±2.0	44.2±1.7	16.1±2.6	0.6	0.4	15.0
			46.2±2.3	31.5±1.9	14.7±3.0	0.6	0.4	13.7
			31.9±2.0	20.2±1.5	11.7±2.5	0.6	0.4	10.7
Cu	29	64.4	73.5±2.6	44.7±1.8	28.8±3.2	0.8	0.7	27.3
			53.8±2.3	31.3±1.7	22.5±2.9	0.8	0.7	21.0
			33.6±1.8	19.0±1.2	14.6±2.2	0.7	0.7	13.2
Nb	41	93	59.0±4.2	29.8±1.9	29.2±4.6	0.9	1.5	26.8
			35.9±3.7	19.0±1.6	16.9±4.0	0.7	1.5	14.7
LF	*	106	103.0	40.2±3.3	62.8±3.3	1.1	2.0	59.8
Ag	47	108.0	53.5±2.4	26.3±1.1	27.2±2.6	1.0	3.5	22.7
			29.7±2.1	16.2±1.1	13.5±2.4	0.7	3.3	9.5
Xe	54	132	84.3±3.9	41.9±1.7	42.4±4.3	1.2	3.0	38.9
			53.7±3.3	28.8±1.6	25.0±3.7	1.0	2.9	21.1
			29.7±4.2	17.6±1.8	12.1±4.6	0.7	2.7	8.7
HF	*	142	78.9	31.1±3.1	47.8±3.1	1.0	3.6	43.3
Au	79	197	75.0±4.8	37.5±1.8	37.5±5.1	1.1	6.4	29.9
			46.8±3.6	26.6±1.5	20.2±3.9	0.8	6.0	13.3
			26.6±3.6	16.1±1.9	10.5±4.1	0.6	5.3	4.6

Table 2. Experimental data of the pulse-height defect in diamond material. Z and A are ion charge and mean value of the mass numbers. E_k is the ion kinetic energy. E_{DD} is the energy measured with the diamond detector. ΔE is the pulse-height defect. ΔE_w, ΔE_r and ΔE_n are the detector entrance window, the nuclear stopping and the residual energy losses, respectively. LF and HF are light and heavy fission fragments of the ^{252}Cf. All energies are given in MeV.

Table 2 shows a summary of the data from our PHD studies in DD. Here Z and A are ion charge and mean value of the mass numbers. E_k is the kinetic energy of the ions incident onto the detector surface, *i.e.* the energy measured with the ToF detectors minus the energy loss in the foil of the second ToF detector. E_{DD} is the energy measured with DD. The total pulse-height defect ΔE is the difference between the kinetic energy E_k deposited in the detector and the energy E_{DD} measured with the diamond detector. ΔE_w is the energy loss caused by the 100 nm aluminium entrance window of the detector. Values of ΔE_w were obtained using the computer code SRIM [21]. The nuclear stopping ΔE_n is the energy loss caused by non-ionizing collisions. It was calculated as described in [2].

$\Delta E_r = \Delta E - \Delta E_w - \Delta E_n$ is the residual energy loss. The abbreviations LF and HF in the first column stand for light and heavy fragment groups from a ^{252}Cf fission source. Kinetic energies of LF and HF are the mean values for the two groups of fission fragments taken from the literature. All energies are given in MeV. These data serve as the basis for the results which are discussed in the following.

3.1 Ion and energy dependence of the PHD

The experimental total PHD for Ti, Cu, Nb, Ag, Xe, Au ions and LF and HF fission fragments of ^{252}Cf is shown in fig. 4 as a function of the kinetic energy in the range from 20 to 105 MeV. As one can see in fig. 4, the PHD in diamond material is significant and increases with increasing ion energy and mass. Literature data on PHD in diamond detectors for comparison with our results do not exist for the studied isotopes and energies.

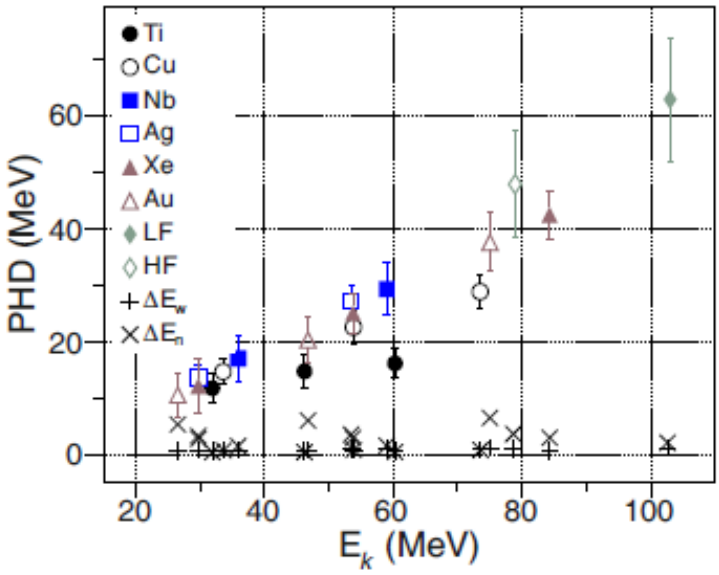

Fig. 4. Pulse-height defect (PHD) *versus* kinetic energy E_k measured with a diamond detector for Ti (•), Cu (o), Nb (■), Ag (□□), Xe (▲), Au (△) ions and for light (◆) and heavy (◊) fission fragments of ^{252}Cf in the energy range (20–105) MeV. ΔE_w is the loss in the detector electrode (+) and ΔE_n is the nuclear stopping loss (×). See details in the text.

In fig. 5 relative PHDs (E_{DD}/E_k) *versus* kinetic energy E_k of the ions are presented. Evidently is the down sloping trend for the two lighter ions Ti and Cu, whereas the heavier isotopes from Nb to Au are inclined upwards. This different trend is a result of the different dependences of the energy loss of the ions on the kinetic energy.

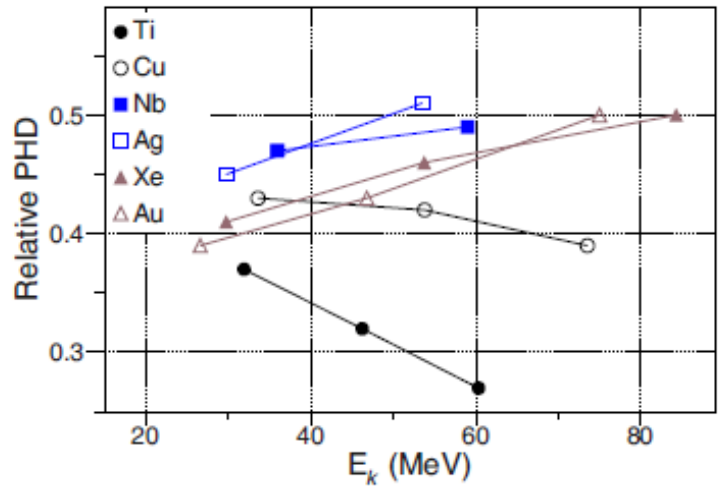

Fig. 5. Relative pulse-height defect (E_{DD}/E_k) *versus* kinetic energy E_k for the same ions as in fig. 4 apart from fission fragments.

Energy losses as function of the energy were calculated using the computer code SRIM [21]. The results for the studied isotopes are shown in fig. 6. The highest energy loss values are reached at the Bragg maximum. According to SRIM it is reached for Ti at an energy of about 55 MeV and for Cu at 90 MeV, whereas the maximum is located at higher energies for the heavier ions. *E.g.* for Nb the Bragg maximum is located at 200MeV and for Ag, Xe and Au at 300, 400, and 650 MeV respectively. From fig. 6 we can see that the energy loss for Ti in the studied energy range (30–60 MeV) increases slowly and has a broad maximum at 55 MeV,

then it starts to decrease resulting in the negative slope of the PHD data shown in fig. 5. Similar is the situation for Cu. But for the rest of the ions, the energy losses are increasing up to the highest energy of 90 MeV studied in this work, which results in the positive slope of their PHD values. As will be discussed in sect. 4.1, electron-hole recombination is the main contribution to the PHD in this energy region. It is highest at the maximum of the Bragg peak where the highest plasma density is produced.

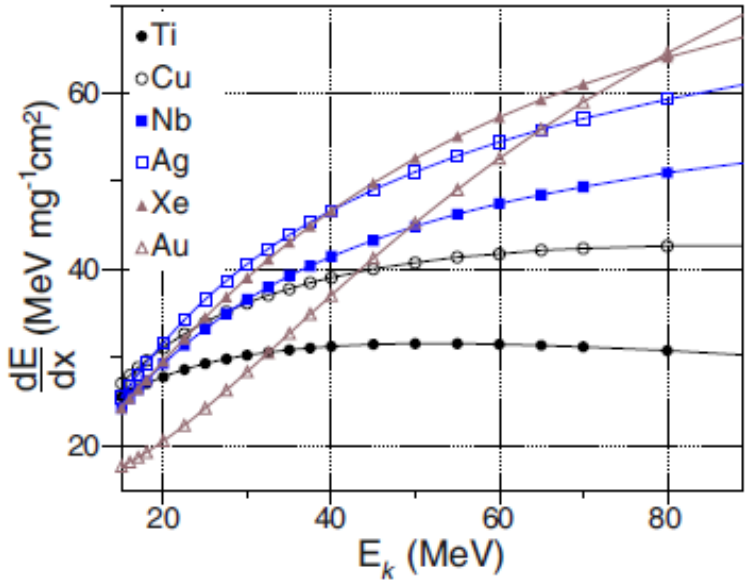

Fig. 6. Calculated energy loss values using SRIM [21] *versus* kinetic energy E_k for the same ions as in fig. 4 apart from fission fragments.

3.2 Electric-field-strength dependence of the PHD

Figure 7 shows the dependence of the peak positions for α particles of ^{226}Ra and fission fragments of ^{252}Cf on the electric field applied to the DD. As one can see, the full charge created by α particles is already collected at an electric field strength of 0.7 V/μm. To check the changes of the peak positions for the fission fragments of ^{252}Cf we applied electric fields of 0.7, 1.0, 2.0, and 2.5 V/μm. As one can see in fig. 7, the charge collection slowly increases towards saturation but it is not yet saturated at 2.5 V/μm. Voltages higher than 250 V (corresponding to an electric field strength of 2.5 V/μm) could not be applied because the preamplifier had no protection against a sudden breakdown current. However, the breakdown electric field for the diamond material is much higher. Values of up to 2000 V/μm can be used, which is $\sim$10 times higher than that for Si.

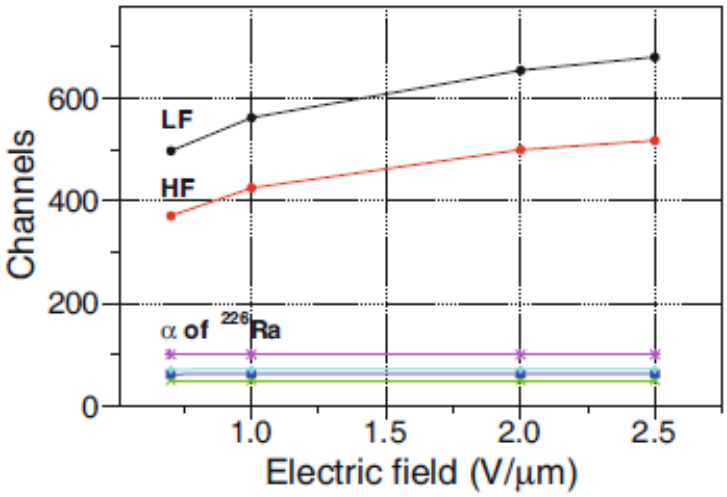

Fig. 7. Peak positions of the diamond detector response E_{DD} as a function of the applied electric field, measured for α particles of ^{226}Ra and for light (LF) and heavy (HF) fission fragments of a ^{252}Cf source.

Table 3 shows the energies of fission fragments of ^{252}Cf measured in the present work with the DD at different electric fields values. At 0.7 V/μm, the PHD is about 70 % of the kinetic energy for HF and LF and about 59 % at 2.5 V/μm. With increasing electric field from 0.7 to 2.5 V/μm, the charge collection increased by $\sim$10%.

Electric field (V/μm)	ΔE (HF) (MeV)	ΔE (LF) (MeV)
0.7	23.6	30.9
PHD (%)	70 %	70 %
1.0	26.8	34.8
PHD (%)	66 %	66 %
2.0	31.3	40.2
PHD (%)	60 %	61 %
2.5	32.1	41.6
PHD (%)	59 %	59 %

Table 3. Energy E_{DD} measured with the diamond detector and corresponding pulse-height defect (in % of the kinetic energy) for HF and LF fission fragments of ^{252}Cf at different electric fields.

4 Discussion

In this section, we are aiming to discuss the physical reasons of the appearance of PHD in DD. A number of calibration methods will be presented, which are typically used for silicon detectors. These calibration procedures were modified in order to get the best agreement with the experimental data obtained in this work. We also work out the systematics of the response of DD to swift ions across a wide mass and energy range.

4.1 Comparison with the recombination models

Reasons of the appearance of PHD were investigated mainly for Si detectors in the past [22–28]. The main process leading to a pulse-height defect is the incomplete charge collection in

the detector. This may arise from various sources, but for heavy ions the main source appears to be the recombination of electron-hole pairs in the plasma bulk produced by the heavily-ionizing particle, first proposed by Miller *et al.* [29]. This process is not as easy to characterize because it may depend on such factors as the applied bias and the distribution of recombination and trapping centers in the detector. Several theoretical studies are aiming to describe the recombination effects in the plasma bulk created by heavily-ionizing particles [22–28]. As a result of many different experiments it was found that the PHD is defined by the sum of three components:

$$\Delta E = \Delta E_w + \Delta E_n + \Delta E_r \quad (2)$$

In eq. (2), ΔE_w is the PHD which corresponds to the energy loss in the entrance window, ΔE_n is the nuclear stopping effect which corresponds to the energy loss in elastic collisions of heavy particles with atoms of the detector material and ΔE_r are residual losses which were proposed to be called the recombination defect. The two first components are generally small and can be easily determined as a correction. The first term is usually defined by the electrode thickness and additional dead layers and the second term can be calculated according to [2]. Concerning the third term, it becomes more complicated since it depends on the applied electric field, particle type and energy and may vary for each detector.

There are few approaches to describe the recombination effect [22,25–28]. The most probable mechanism of charge losses in measurements with heavily-ionizing particles is the recombination of created electron-hole pairs in a dense plasma track [29]. Finch *et al.* [22] proposed to use the formula

$$\Delta E_r = \frac{5.10^{11}\ E_k\,(dE/dx)^2}{\tau_0\ \varepsilon^2} \quad (3)$$

Here, E_k is the deposited energy in MeV, dE/dx is in MeV/(mg . cm^{-2}), τ_0 is the lifetime in μs of the non-equilibrium carriers at low excited level which can be adjusted as reasonable value, ε is the electrical field in V/cm. Adjusted values of τ_0 could satisfactorily describe the experimental data. Nevertheless, the PHD calculations made via eq. (3) overestimate the PHD at higher electric field and underestimate it at low electric field, respectively.

The recombination mechanism was studied further in [26–28]. This study is based on the recombination Shockley-Read-Hall model [30,31]. According to this model, the recombination of carriers occurs in the volume of the dense plasma track and on its surface [26]. Authors in [27] suggested that surface recombination plays the main role in recombination. Akimov *et al.* [28] summarized the previous knowledge and propose to calculate the PHD with the following equation.

$$\Delta E_r = k\frac{\sqrt[3]{Z^2}\,E_k}{R}\,t_p \quad (4)$$

where t_p is the plasma time which is the time needed to erode the plasma to the point where all charges are under the influence of the electric field [32–34], R is the range and k is an adjusted coefficient. The value of k was determined for Cu, Ag, I, Xe, Au, and U and is equal to $(8.0 \pm 0.6) \times 10^{-3}$ μm/ns [28]. Thus, eq. (4) is taking into account the volume and surface effects and fulfils the experimental dependences on (E, Z, R).

The recombination losses depend on (E, Z, R) on the one hand and on the applied electric field and properties of the given detector (material, construction features, etc.) on the other hand.

According to Finch *et al.* [22–24] the relative recombination energy losses λ can be calculated as

$$\lambda = \frac{\Delta E_r}{E_k} = \frac{t_p}{\tau_0} \quad (5)$$

where t_p is the plasma time and τ_0 is the carrier lifetime which is the average time needed by the excess carriers to recombine. According to Seibt *et al.* [32,33] the plasma time can be calculated as

$$t_p = \frac{1}{F} \sqrt[3]{\frac{3\, Q_0\, q\, n_1\, A}{32\, \pi^3\, \mu\, (\epsilon\, \epsilon_0)^2\, D_a^2}} \quad (6)$$

where Q_0 is the total created charge, q is the electric charge, μ is the carrier mobility, ϵ is the relative dielectric constant for the detector material, ϵ_0 is the permittivity of a free space, D_a is the ambipolar diffusion constant for the detector material, n_1 is the linear concentration of created carriers. The area A is defined by the spot of the incoming beam. F is the electric field strength. It is convenient to introduce the deposited energy E_d instead of Q_0. Since 13 eV are required to form an electron-hole pair in diamond we finally get the expression

$$t_p = \frac{3.07 \times 10^{-11}}{F} \sqrt[3]{n_1 E_k} \quad (7)$$

where we also used μ = 2700 cm/Vs and D_a = 97cm^2/s obtained from [35]. The area A was given the value 3.14×10^{-8} cm^2 which corresponds to a plasma track with radius r = 1 μm [32,33]. The values for the plasma time calculated via eq. (7) are around 1 ns at the applied in our experiment electric field of 2 V/μm. The resulting plasma time t_p *versus* deposited energy E_k is presented in fig. 8 at 2 V/μm applied in our experiment, and at 1.0 and 3.0 V/μm for comparison. The plasma time depends on the ion energy and electric field but it does not depend on the ion mass. The deviations for different masses are not more than 10 %. For comparison, in Si detectors the plasma time is about (10–20) ns and deviations are not more than (5–6) % for fission fragments.

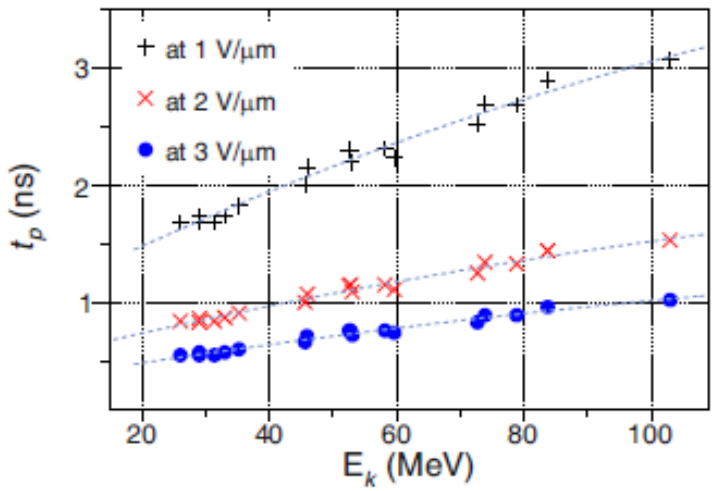

Fig. 8. Plasma time for the diamond detector *versus* kinetic energy E_k determined according to Seibt *et al.* [33] at 1.0, 2.0 and 3.0 V/μm. Lines are for eye guiding.

Recent studies of charge-carrier properties of DDs show that the carrier lifetime is about few hundreds of nanoseconds or even more [20,35]. One can estimate the carrier lifetime with eq. (5) inserting the plasma time obtained with eq. (7). The resulting carrier lifetimes are about

(1–10) ns, which is on the same order as the carrier lifetimes for polycrystalline CVD diamonds [20,35].

The resulting values are close to 1 ns which is ~ 10 times smaller than that in Si detectors and seems to be reasonable because carrier mobility and ambipolar diffuseness are higher in diamonds. Probably, the plasma created by an incoming heavily-ionizing particle produces temporal traps in the diamond bulk which influence the charge collection process. Another studies show that a possible reason for such high PHD in diamond could be the formation of excitons which is proportional to the ionization density [36]. A question which needs to be studied in more detail.

We considered recombination losses as proposed by Akimov *et al.* [28] taking into account the plasma time (eq. (7)). However, the calculated values for the PHD with parameter k = 0.008 (suitable for Si [28]) do not fit our experimental data. There is no single parameter k which fits all experimental data simultaneously. Since this parameter depends on ion mass and energy, we represent it as a next function:

$$k(E,Z,R) = 0.25 - 0.26 \times \exp\left(-\frac{R(E)}{(0.045\times Z)^2}\right) \quad (8)$$

In this case, we get a very good agreement with our experimental data. Figure 9 presents the PHD calculated with eq. (4) and the parameter k calculated as a function of (E, Z, R) with eq. (8). Finally, the theoretical approach to calculate the PHD, proposed by Akimov and co-authors, taking into account the plasma time according to eq. (7) with the modified parameter k as a function of (E, Z, R) (eq. (8)) fits the experimental data of PHD in diamond material very well as presented in fig. 9.

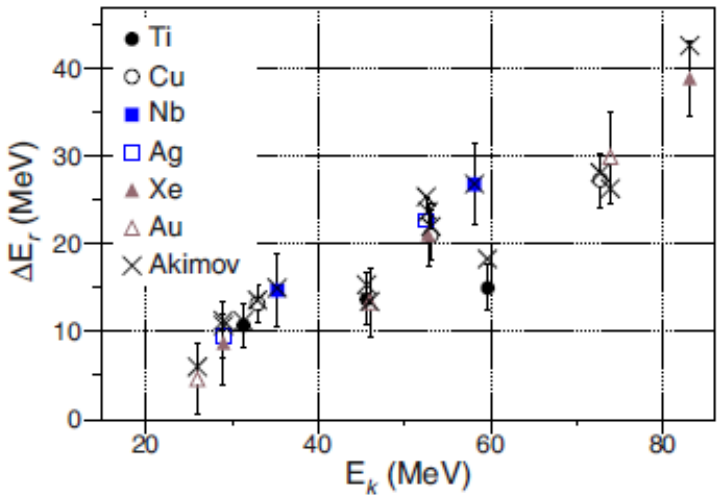

Fig. 9. Experimental pulse-height defect in the diamond detector *versus* kinetic energy E_k calculated according to Akimov *et al.* (eq. (4)) with the parameter a as a function of (E, Z, R), eq. (8).

4.2 Empirical calibrations

Empirical calibration methods were investigated at the same time with recombination studies [1–6]. Here we are going to discuss some of them.

4.2.1 The method of Schmitt et al.

The most widely-used technique has been proposed by Schmitt *et al.* [1]. Experimental data on PHD in surface-barrier silicon detectors show that the response of those detectors to ions in the mass and energy range of fission fragments ($A \approx$ (80–150) a.m.u, $E \approx$ (35–120) MeV) is linear and mass-dependent. The calibration method of Schmitt *et al.* was based on combined measurements of the response of silicon semiconductor detectors to the single ^{252}Cf spontaneous fission fragments with ions of bromine and iodine, and was expressed by the following equation:

$$E(x, A) = (a + a'A)x + b + b'A \quad (9)$$

where E is the calibrated energy, A is the ion mass, x is the channel number and a, a', b, b' are parameters. The channel numbers of the peak positions for the average light and heavy fission fragment groups, X_l and X_h, respectively, were then related to the four parameters in eq. (9), which are presented in table 4, so that a measurement of one of the standard fission spectra sufficed to determine these parameters.

Parameter	^{252}Cf	^{235}U
a	$\frac{24.0203}{X_l - X_h}$	$\frac{30.9734}{X_l - X_h}$
a'	$\frac{0.03574}{X_l - X_h}$	$\frac{0.04596}{X_l - X_h}$
b	$89.6083 - a\,.X_l$	$87.8626 - a\,.X_l$
b'	$0.1370 - a'\,.X_l$	$0.1345 - a'\,.X_l$

Table 4. Parameters of eq. (9) (in MeV) for fission fragments of ^{252}Cf and ^{235}U.

We applied and checked this method for diamond detectors. The Schmitt calibration requires to determine the parameters a, a', b, b' in eq. (9). For this, we measured fission spectra of ^{252}Cf and determined the respective channel numbers, X_l and X_h, which correspond to the maxima of the light and heavy fission fragment groups, respectively. Then, taking into account the equations in table 4 we determined a, a', b, b'. Finally, we considered that the maxima correspond to fission fragments with light M_L = 106 and heavy M_H = 142 mass, respectively (typical mass numbers for fission fragment groups of ^{252}Cf), and calibrated their energy according to eq. (9). The obtained energy values of LF and HF are shown in table 5 and compared with literature values [1, 37]. The reconstructed energies are very close to the values for fission fragments measured with Si detectors in [1, 37].

Ion	E (HF) (MeV)	E (LF) (MeV)
Present work	79.9	104.1
[1]	79.4	103.8
[37]	78.9	103.0

Table 5. Reconstructed energies of light (LF) and heavy (HF) fission fragments of ^{252}Cf, measured with the diamond detector and comparison with literature values from measurements with Si detectors. The energy calibration was performed with the method of Schmitt *et al.* The LF and HF energies correspond to fission fragments with mass M_L = 106 and M_H = 142, respectively, which are located at the maxima of the fission fragment peaks.

It has to be mentioned that for the best fit, the constants in the equations in table 4 have to be adjusted for the given detector (as described in [37]) otherwise the calibrated energies might be over- or underestimated. We conclude that the reconstructed energies of HF and LF fission fragments of ^{252}Cf are in good agreement with the literature values. The calibration method of

Schmitt *et al.* works in fission fragment mass and energy regions for diamond detectors as well as for Si detectors.

Concerning the ion beams investigated in our experiment, only Ag at the energy of 53.5 MeV and Xe at energies 84.3 and 53.7 MeV fulfill the required range. However, the conditions of our electronics were not the same during the measurements with ions and with fission fragments. Therefore, we could not apply the calibration method of Schmitt for Ag and Xe ions.

Although the Schmitt method has been used successfully in the fission fragment range of masses and energies, its originators warned that this calibration method may not be valid outside of this range.

4.2.2 The method of Moulton et al.

Later, Moulton *et al.* [4] developed one more calibration method based on studying the PHD with ions from Ne to Au in a wide energy region (5–160MeV). It has to be mentioned that contrary to the authors who defined the PHD as the difference between the true energy of an ion incident on a detector and its apparent energy, they propose to use another definition

$$\Delta E = (E_k - \Delta E_w) - E_{DD} = E_d - E_{DD} \quad (10)$$

where ΔE_w means the energy loss in the entrance window of the detector. To define the PHD, the following dependence was obtained:

$$\Delta E = 10^f E_d^g \quad (11)$$

where g and f are parameters, g is the slope and f is the y-intercept of a plot of log PHD *versus* log E_d. Both, the slopes and the intercepts, increase with atomic number Z. It turned out that these constants depend on Z (or mass number A):

$$g(Z) = 0.02230\ (Z^2/10^3) + 0.5682 \quad (12)$$

$$f(Z) = -0.1425(100/Z) + 0.0825 \quad (13)$$

or

$$g(A) = 0.03486\ (A^2/10^4) + 0.5728 \quad (14)$$

$$f(A) = -0.2840\ (100/A) + 0.0381 \quad (15)$$

Examples of g and f for Au and Xe can be found in table 6; they were obtained only for one given Si detector and at one given value of the electric field.

For the calibration method proposed by Moulton and co-authors we considered that the energy deposited in the detector E_d is the incident kinetic energy E_k after subtracting the energy loss ΔE_w in the electrode [4]. The PHD obtained with eq. (11) is presented in fig. 10 as a function of deposited energy. There is no (g, f) parameter set which gives us a good agreement with all experimental data at once. The best fit is obtained with $g = 1.09$, $f = -0.54$ (dashed line (2) in fig. 10).

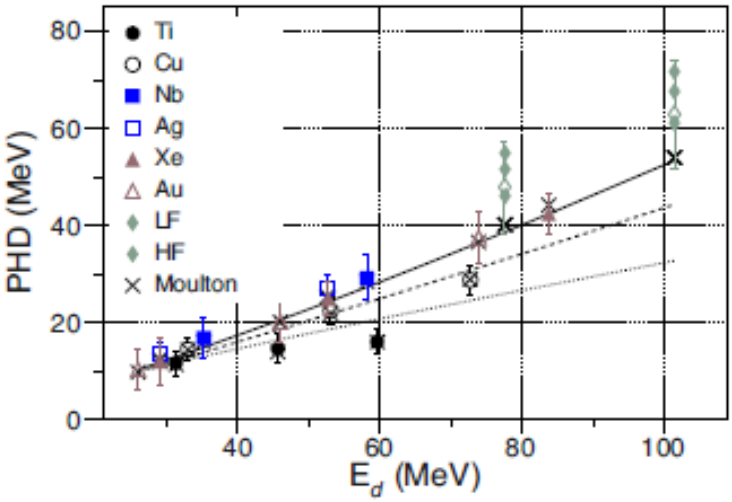

Fig. 10. Experimental pulse-height defect (PHD) in the diamond detector *versus* deposited energy E_d. Dotted line (1): PHD calculated by eq. (11) with $g = 0.86$, $f = -0.21$; dashed line (2): with $g = 1.09$, $f = -0.54$; solid line (3): with $g = 1.2$, $f = -0.68$. The PHD calculated by eq. (11) with $g(Z)$ and $f(Z)$, eqs. (16), (17) (or $g(A)$ and $f(A)$, eqs. (18), (19)) is represented by crosses.

For heavy and light ions, values of g and f can be used as follows: $g = 1.2$, $f = -0.68$ for the heavy ions Au, Xe, Nd and fission fragments (solid line (3) in fig. 10) and $g = 0.86$, $f = -0.21$ for the light ions Ti and Cu (dotted line (1) in fig. 10). It turned out that the proposed eqs. (12)–(15) for $g(Z)$ and $f(Z)$ (or $g(A)$ and $f(A)$) are not suitable for diamond detectors. Instead, we found the following dependences:

$$g(Z) = 1.26 - 5.71 \times 0.91^{Z} \quad (16)$$

$$f(Z) = -0.79 + 5.81 \times 0.93^{Z} \quad (17)$$

or

$$g(A) = 1.25 - 5.09 \times 0.96^{A} \quad (18)$$

$$f(A) = -0.79 + 5.19 \times 0.97^{A} \quad (19)$$

With them, we got very good agreement with experimental data. The resulting PHD values are represented by crosses in fig. 10. The calculated PHDs for LF and HF fission fragments of ^{252}Cf by eq. (11) with $g(Z)$ and $f(Z)$, eqs. (16), (17) (or $g(A)$ and $f(A)$, eqs. (18), (19)) underestimate the experimental data which are represented for different electric fields by diamonds in fig. 10.

4.3 Comparison with Si data

Figure 11 shows a comparison of the PHD in CVD diamond material with the PHD in Si detectors for Cu, Ni, Ag, and Au ions in the energy region E = (20–90) MeV. Lighter particles like Cu and Ni have a more significant PHD in diamond material as well as heavier ions like Ag. Concerning Au, the heaviest ion in our experiment, the PHD, is similar in DD and silicon in the low-energy region up to 40 MeV. At higher energies from 40 to 90 MeV, the PHD in diamond material is more significant than in Si. In fig. 11 the data presented for Au in Si are from two different experiments [2,4]. In both experiments surfacebarrier detectors for heavy ions made by ORTEC were used. The difference was the following: in [2] authors used the Si detector (ORTEC 7408) with a sensitive thickness of 80 μm and a resistivity of 380 ohm cm

at operating bias of 70 V; in [4] authors used the detector (ORTEC 15-016C) with a sensitive thickness of 300 μm and a resistivity of 1000 ohm cm at an operating bias of 150 V.

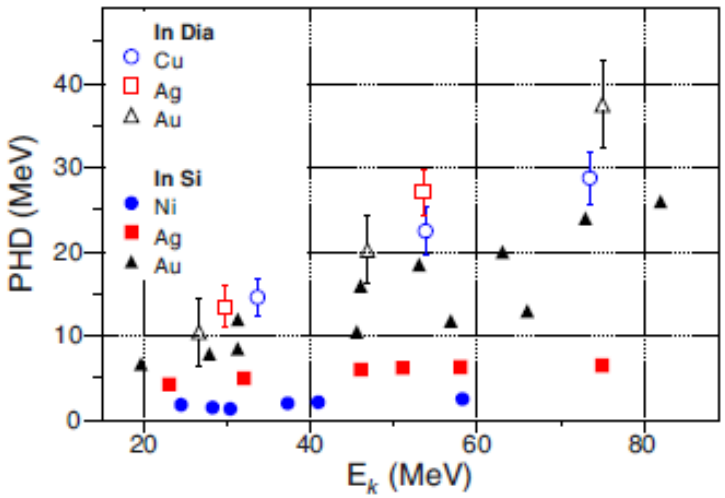

Fig. 11. Comparison of the pulse-height defect in the diamond detector (present work) and in silicon [2, 4] in the energy region (20–90) MeV. The presented data for Au in Si are from two different experiments.

5 Summary and conclusions

We studied experimentally the pulse-height defect (PHD) in single-crystal CVD diamond detectors (DD) for slow heavy ions (Ti, Cu, Nb, Ag, Xe, and Au) with energies in the range (20–90) MeV. A significant effect was measured for these low-energy ions in contrast to fully-ionized relativistic heavy ions where the charge collection was found to be close to 100%.

We analyzed the data measured with the DD in the framework of recombination models which take into account the contribution of residual recombination losses to the PHD. We calculated the plasma time in diamond as a function of the deposited energy and found it to be about 10 times smaller than that in silicon. The parameter for the recombination part of the PHD was modified as a function of ion energy, proton number, and range of the ion in DD. The obtained results are in good agreement with our experimental data.

To quantify the PHD in DD for slow ions, we adapted and applied two different empirical calibration methods, which are usually used to determine the PHD in silicon detectors.

1) We used the method of Schmitt *et al.*, which works well in the mass and energy range of fission fragments, to determine the PHD of fission fragments from ^{252}Cf in DD. We found that this calibration method works in the fission fragment mass and energy range for diamond detectors as good as for Si detectors. However, constants have to be adjusted for diamond material, otherwise the reconstructed energies might be slightly over- or underestimated.
2) Also with the method of Moulton *et al.*, we had to adjust the calibration parameters for the diamond material. New dependences of the parameters as a function of Z (or A) were obtained. Also here, the calculated PHD shows a satisfactory agreement with experimental data.

Our experiment revealed that the PHD in diamond for low-energetic ions is significant and amounts up to the values of $\sim 50\%$ for heavy ions in the energy range of (20–90) MeV. A comparison with data for PHD in Si detectors showed that the PHD in diamond material is higher than that in Si for the same ion type and energy. A possible reason for this high PHD in diamond could be the formation of excitons which is proportional to the ionization density. A question which we are planning to study in further experiments.

While the studies of PHD in Si detectors have a long history and many experimental data are available, the investigation of the PHD in CVD diamond detectors for low-energetic ions is only at its very beginning. More experimental data are needed in order to measure more details of the response of DDs on the stopping of such ions. Also studies of the radiation hardness and timing properties for low-energetic heavy ions will be the subject of future investigations.

References

1. H.W. Schmitt, W.E. Kiker, C.W. Williams, Phys. Rev. **137**, B837 (1965).
2. B.D. Wilkins *et al.*, Nucl. Instrum. Methods **92**, 381 (1971).
3. S.B. Kaufman *et al.*, Nucl. Instrum. Methods **115**, 47 (1974).
4. J.B. Moulton *et al.*, Nucl. Instrum. Methods **157**, 325 (1978).
5. B.M. Golovin, V.P. Kushniruk, L.A. Permiakova, Preprint of JINR **15-82520** (1982) (in Russian).
6. S.I Mulgin, V.N Okolovich, S.V Zhdanov, Nucl. Instrum. Methods **388**, 254 (1997).
7. M. Pomorski *et al.*, Phys. Status Solidi (a) **202**, 2199 (2005).
8. M. Pomorski *et al.*, Phys. Status Solidi (a) **203**, 3152 (2006).
9. M. Friedl, Diploma Thesis, University of Technology, Vienna, 1999, http://www.hephy.at/user/friedl/da/da.pdf.
10. C. Bauer *et al.*, Nucl. Instrum. Methods **383**, 64 (1996).
11. A. Oh, M. Moll, A. Wagner, W. Zeuner, Diam. Relat. Mater. **9**, 1897 (2000).
12. E. Berdermann *et al.*, Diam. Relat. Mater. **17**, 1159 (2008).
13. Y. Sato *et al.*, EPL **104**, 22003 (2013).
14. Y. Sato, H. Murakami, Jpn. J. Appl. Phys. **54**, 096401 (2015).
15. M.O. Fregeau *et al.*, Nucl. Instrum. Methods A **791**, 58 (2015).
16. O. Beliuskina *et al.*, GSI scientific report, 2013, DOI:10.15120/GR-2014-1-NUSTAR-SHE-07.
17. M. Rejmund *et al.*, Nucl. Instrum. Methods A **646**, 184 (2011).
18. E.M. Kozulin, N.A. Kondratjev, I.V. Pokrovski, Scientific Report 1995-1996, JINR, FLNR, Dubna (1997).
19. M.G. Itkis *et al.*, Phys. Rev. C **59**, 3172 (1999).
20. Element Six, *The Element Six CVD Diamond Handbook*, see www.e6.com.
21. J.F. Ziegler, J.P. Biersack, M.D. Ziegler, *SRIM-2013.00, The Stopping and Range of Ions in Matter* (2013) http://www.SRIM.org.
22. E.C. Finch, Nucl. Instrum. Methods **113**, 41 (1973).
23. E.C. Finch *et al.*, Nucl. Instrum. Methods **142**, 539 (1977).
24. E.C. Finch, M. Ashgar, M. Forte, Nucl. Instrum. Methods **163**, 467 (1979).
25. M. Ogihara *et al.*, Nucl. Instrum. Methods A **251**, 313 (1986).
26. V.K. Eremin, N.B. Strokan, N.I. Tisiek, Phys. Tech. Semicond. **10**, 58 (1976) (in Russian).
27. V.P. Kushniruk, Preprint of JINR **13-11933, 13-11889** (in Russian) (1978).

28. Yu.K. Akimov *et al.*, *Semiconductor Detectors in Experimental Physics* (Energoatomizdat, 1989) p. 87 (in Russian).
29. G.L. Miller *et al.*, IRE Trans. Nucl. Sci. **1NS-7**, 185 (1960).
30. W. Shockley, W.T. Read jr., Phys. Rev. **87**, 835 (1952).
31. R.N. Hall, Phys. Rev. **87**, 387 (1952).
32. P.A. Tove, W. Seibt, Nucl. Instrum. Methods **51**, 261 (1967).
33. W. Seibt, K.E. Sundstroem, P.A. Tove, Nucl. Instrum. Methods **113**, 317 (1973).
34. R.N. Williams, E.M. Lawson, Nucl. Instrum. Methods **120**, 261 (1974).
35. E. Gaubas *et al.*, Sensors **15**, 13424 (2015).
36. N. Naka, H. Morimoto, I. Akimoto, Phys. Status Solidi (a) **213**, 2551 (2016).
37. G.N. Knyazheva *et al.*, Nucl. Instrum. Methods B **248**, 7 (2006).